MOLECULAR STRUCTURE AND VIBRATIONAL SPECTRA OF OF 3-(4-METHOXYBENZOYL)PROPIONIC ACID

T.CHITHAMBARATHANU, K.VANAJA, J.DAISY MAGDALINE

Abstract: The FT-IR and FT-Raman spectra of 3-(4-methoxybenzoyl) Propionic acid have been analyzed in the region 4000-450 and 4000-50cm^{-1}respectively. The geometrical structure, harmonic vibrational frequency, infrared intensity, Raman activities and bonding features of the title compound were carried out by (HF) with 6-31G (d, p) and DFT (B3LYP) with 6-31++G (d, p) and 6-311++G (d, p) basis sets.The complete vibrational frequency assignments were made by normal co-ordinate analysis following the scaled quantum mechanical force field methodology (SQM). The charge transfer and hyperconjugative interactions have been analyzed using natural bond orbital (NBO) analysis. The calculated HOMO-LUMO energy gap shows that charge transfer occurs within the molecule. The reactivity sites are identified by mapping the electron density into electrostatic potential surface (MESP).

Keywords:DFT, HOMO-LUMO, 3-(4-methoxybenzoyl) Propionic acid, NBO.

Introduction: Propionic acid (PA) and its derivatives are largely used as feed and food derivatives. Antimicrobial feed additives such as PA is effective to antibiotic growth promoters for safe animal products as well as human health. Propionic acid is also useful as a chemical intermediate. It can be used to modify synthetic cellulose fibres. It is also used to make pesticides and pharmaceuticals.The propionic acid inhibits the growth of moulds and some bacteria [1]. The esters of PA are sometimes used as solvent or artificial flavourings [2]. Physicians commonly prescribe the formulation for breast cancer and hormone replacement therapy. Derivatives of propionic acid such as ibuprofen and fenoprofen are widely used in the pharmaceutical industry [3]. Ibuprofen is used for inflammatory diseases such as juvenile idiopathic arthritis and rheumatoid arthritis [4]. In the progressive studies of propionic acid herein 3-(4-methoxybenzoyl) propionic acid (MBPA) has been taken as the object of spectral, structural and theoretical investigations because of its interesting physicochemical and biological properties. The complete vibrational analysis of MBPA was performed by combining the experimental (FT-IR and Raman) and theoretical information using Pulay's density functional theory (DFT) based on the scaled quantum mechanical (SQM) method.

Experimental Details: The compound 3-(4-methoxybenzoyl) propionic acid in the solid form is purchased from the Sigma Aldrich Chemical Company (USA) with a stated purity of 98% and used as such without further purification. The FT-Raman spectra are recorded in the range of 4000-50 cm^{-1} using the BRUKER, Model RFS 100/s FT-Raman spectrophotometer. The FT-IR spectrum of the sample is recorded using Perkin Elmer RXI spectrometer in the region 4000-450 cm^{-1} in the evacuation mode using KBr pellet technique.

ComputationalMethods: The quantum chemical calculations of MBPA have been performed using Gaussian 03 program package [5] at the ab-initio (HF) and Becke 3-Lee-Yang-Parr (B3LYP) methods. The molecular geometry, optimized parameters and vibrational frequencies are computed by performing both ab-initio (HF) with 6-31G (d, p) and DFT(B3LYP) with 6-31++G(d, p) and 6-311++G(d, p)basis sets. The scaling of the force field is performed according to the scaled quantum mechanical procedure (SQM) [6] using selective scaling in the natural internal co-ordinate representation to obtain a better agreement between the theory and the experiment. Normal co-ordinate analyses have been performed in order to obtain the detailed interpretation of the fundamental modes using the MOLVIB program version 7.0 written by Sundius [7]. The NBO calculations [8] are performed using NBO 3.1 program as carried out in the Gaussian 03 W package at the DFT/B3LYP level in order to understand the various second order interactions between the filled orbitals of one sub system and the vacant orbitals of another sub system, which is a measure of delocalization or hyper conjugation.

Results and discussion: Molecular geometry: Optimized geometric parameters of MBPA calculated by the HF/6-31G (d, p), B3LYP/6-31++G (d, p) and B3LYP/6-311++G (d, p) basis sets are listed in Table I. The optimized structure of MBPA with labeling atoms is shown in Fig.1. The optimized geometric parameters of MBPA are compared with the experimental XRD data [9] of the title molecule. In the title molecule, the introduction of two substituent groups on the benzene ring causes some changes in the C-C bond lengths at the position of the substituents. The hexagonal symmetry of the benzene ring is obvious from the bond lengths of the C7-C12 and C10-C11 bonds. The magnitudes of the C7-C12 and C10-C11 bonds are found to be 1.406 Å and

1.402 Å respectively, which is slightly bigger than the double C=C bond length but shorter than the single C-C bond length. J. Tonannavar et al. [10] and Zhang Rui- Zhou et al. [11] reported C=O and C-O bond lengths in the carboxylic group as 1.204, 1.349 Å and 1.207, 1.347 Å for the compounds 2-bromo-3-phenyl propionic acid and N-benzoyl glycine. For the compound MBPA, the C=O and C-O bond lengths are found to be 1.199 and 1.363 Å. The bond length C1-O5 (1.363 Å) in the carboxylic group of MBPA is elongated when compared to the bond length C-O (1.347 Å) in N-benzoyl glycine [15], C-O (1.353 Å)in ketoprofen[12] and C-O (1.348 Å) in 2-chlorobenzoic acid[13]. This is due to the presence of methylene groups.The bond lengths C7-C6 (1.489Å), C6-C3 (1.524Å), C2-C3 (1.524Å) and C2-C1 (1.519Å) calculated by the B3LYP/6-311++G (d, p) methodis in good agreement with the reported values for the compoundfenbufen [14].

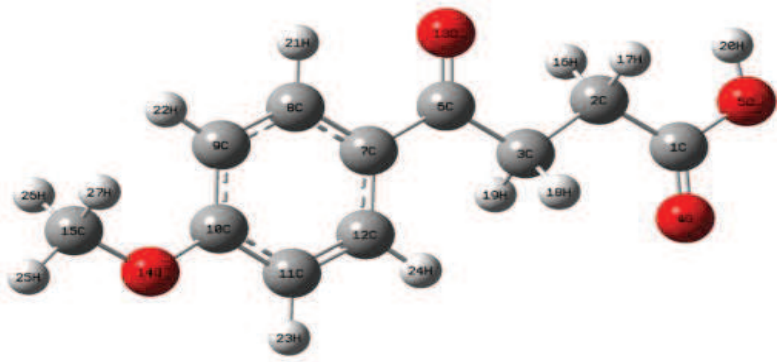

Fig.1 Molecular structure with atom numbering of MBPA.

Table IExperimental (XRD) and optimized geometrical parameters of MBPA computed at HF/6-31G(d, p), B3LYP/6-31++G (d, p) and 6-311++G(d, p) basis sets

Bond length	Bond lengths(Å)			
	Experimental value	HF/6 31G (d, p)	B3LYP/6 31++G(d, p)	B3LYP/6-311++G(d, p)
C1-C2	1.491	1.513	1.519	1.519
C1-O4	1.229	1.183	1.207	1.199
C1-O5	1.301	1.334	1.364	1.363
C2-C3	1.511	1.521	1.525	1.524
C3-C6	1.508	1.518	1.525	1.524
O5-H20	0.820	0.944	0.969	0.965
C6-C7	1.478	1.491	1.489	1.489
C6-O13	1.220	1.199	1.228	1.221
C7-C8	1.384	1.388	1.403	1.399
C7-C12	1.397	1.397	1.409	1.406
C8-C9	1.383	1.383	1.392	1.389
C9-C10	1.379	1.390	1.405	1.402
C10-C11	1.395	1.394	1.405	1.402
C10-O14	1.352	1.341	1.359	1.357
C11-C12	1.370	1.375	1.387	1.384
O14-C15	1.426	1.402	1.426	1.425

Vibrational Spectral Analysis: The vibrational spectral assignments of MBPA have been carried out with the help of normal coordinate analysis. The detailed vibrational spectral assignments of the experimental wavenumbers are based on normal mode analyses and a comparison with theoretically scaled wavenumbers with PED by HF and B3LYP methods. The observed and scaled theoretical frequencies using the HF/6-31G (d, p), B3LYP/6-311++G (d, p) and B3LYP/6-31++G (d, p) basis sets

with PEDs are shown in Table II. The experimental (FT-IR and FT-Raman) and simulated vibrational spectra of MBPA are displayed in Fig.2.

C-H vibrations: In disubstituted benzenes, the four C-H stretching vibrations fall in the range 3100-3000 cm^{-1} [15]. In this region, these vibrations are not found to be affected by the nature and position of the substituent [16]. Mehmet Karaback et al. [17] observed the C-H stretching vibrations in the region 3097-3058 cm^{-1}**.** In MBPA, the FT-IR bands at 3104, 3070 and 3051 cm^{-1} and the FT-Raman bands at 3106 and 3063 cm^{-1} have been assigned to C-H stretchingvibrations. Most of the C-H stretching modes are found to be weak which is due to the charge transfer from the hydrogen atoms to the carbon atoms. The C-H stretching vibrations are calculated at 3168, 3079, 3068 and 3060 cm^{-1} by the HF/6-31 G(d, p) method and at 3207, 3077, 3066 and 3059 cm^{-1} by the B3LYP/6-31++G (d, p) method and at 3077, 3066, 3059 and 3051 cm^{-1} by the B3LYP/6-311++G (d, p) method. The C-H in-plane bending vibrations usually occur in the region 1300-1000 cm^{-1} and these vibrations are very useful for characterization purposes [18]. The C-H out-of-plane bending frequencies appear in the rangeof 1000-750 cm^{-1} [19]. Sundaraganesan et al. [13] assigned the C-H in-plane and out-of-plane bending modes in the region 1255-1103 cm^{-1} and 950-809 cm^{-1} respectively for the compound 2-chlorobenzoic acid. The C-H in-plane vibrations for the title compound are computed theoretically at 1302, 1285, 1150, 1098 and at 1288, 1268, 1173, 1100 cm^{-1} and at1296, 1272, 1159, 1109 cm^{-1} by the HF/6-31G (d, p), B3LYP/6-31++G (d, p) and B3LYP/6-311++G (d, p) methods respectively. The peaks at 1298, 1266, 1161

Table IIComparison of the experimental (FT-IR and FT-Raman) wavenumbers (cm^{-1}) and theoretical wavenumbers (cm^{-1}) of MBPA calculated by HF/6-31G (d,p), B3LYP/6-31++G (d, p) and B3LYP/6-311++G (d, p) basis sets

Observed Wavenumbers (cm^{-1})		Calculated by HF/6-31G(d, p)			Calculated by B3LYP/6-31++G(d, p)			Calculated by B3LYP/6-311++G(d, p)			Characterization of normal modes with PED (%)[c]
IR	Raman	Scaled waavenumbers (cm^{-1})	A_iIR^a	I_iR_b	Scaled waavenumbers (cm^{-1})	A_iIR^a	I_iR^b	Scaled waavenumbers (cm^{-1})	A_iIR^a	I_iR^b	
3318(w)	-	3318	87	41.4	3318	44.3	62.5	3318	50.1	69.8	υOH(100)
3104(w)	3106(w)	3168	30	118	3207	14.8	118.5	3077	8.3	121.8	υCH(99)
3070(w)	3063(w)	3079	10	109	3077	10.4	1258	3066	3.6	126.6	υCH(99)
3051(w)	-	3068	7.1	110	3066	4.6	129.8	3059	0.03	41	υCH(98)
-	-	3060	4	43.7	3059	0.3	38.3	3051	3.5	40	υCH(98)
3028(w)	3029(w)	3046	8	44	3050	5.5	43.4	3049	16.3	124	CH3ips(94)
2966(w)	2985(w)	2966	14.4	6.5	2966	9	10,2	2966	6.6	8.6	CH2ASS(87),CH2AS1(12)
-	2954(w)	2951	15.3	46.4	2948	36	63.7	2956	19.1	70.2	CH2SS(98)
2948(w)	-	2948	50	45.2	2936	2.9	71.6	2948	31.5	59.8	CH3ops(100)
2936(w)	-	2936	2.8	76.9	2926	28.8	3.4	2936	2.2	61	CH2AS1(87),CH2ASS(13)
2917(w)	2921(m)	2917	10.6	86.6	2917	0.4	170.2	2917	9.9	121.7	CH2SS1(98)
2841(w)	2841(w)	2841	52.6	128	2841	57.3	176.5	2841	56	192.4	CH3SS(96)

1695(s)	-	1695	239.9	7.6	1695	168.9	17.2	1695	185.4	19.9	COd2S(79)
1674(w)	1665(s)	1665	148.3	7.1	1674	375.8	274.3	1674	256.9	135.1	COdS(74),βCCC(6)
1599(s)	1605(s)	1630	294.3	183	1599	220.6	123.8	1596	323.7	299.8	υCC(61), βCH(19)
1574(s)	1576(s)	1606	108.2	52.6	1574	17.6	18.3	1574	20.1	15.3	CH3ipb(94)
1565(s)	-	1572	7.8	25	1551	10.2	11.2	1551	7.6	6	υCC(67), βCH(11)
1514(s)	1515(w)	1514	135.6	2.2	1514	66.1	19.5	1510	50.1	4.3	υCC (42), βCH (32)
1464(m)	1463(w)	1465	16.5	13.8	1464	35.5	13.8	1464	31.4	10	CH3opb(89), CH3ipr(8)
1425(s)	1439(w)	1435	2.4	10.1	1435	32.1	6.5	1435	1.9	5.1	CH3sb(87), βCH(5)
1406(s)	1406(w)	1411	12.9	1.2	1406	11.6	4.7	1406	12.8	3.2	CH2SC(83)
1396(s)	1396(w)	1405	1	3.1	1397	58.3	3.2	1402	10.6	1.8	υCC(49), βCH(34)
1361(s)	-	1379	0.8	5	1360	14.3	5	1361	15.6	3.7	CH2wag1(66), υCC1(17)
1317(m)	1320(w)	1319	15.4	1.7	1320	304.2	6.3	1323	347.1	48.3	υCC(25), CCar(22)
1302(m)	-	1313	3.9	11.4	1302	137.8	15	1302	0.3	6.9	CH2tw1(84), CH2tw(7)
1298(m)	-	1302	467.7	39.8	1288	0.2	8.5	1296	16.9	1.1	βCH(36), υCC(31)
1266(m)	1269(w)	1285	6.8	15.3	1268	19	11.5	1272	87.7	18.2	βCH (44), υCC (28)
1246(s)	1245(s)	1245	172.7	38	1246	121.5	13.5	1247	149.9	10.7	υCO(41), υCC(28)
1240(w)	-	1243	428.4	3.4	1241	396	6.2	1242	190.6	2.7	CH2sc1(73), βHOC(10)
1189(s)	1190(m)	1197	24.4	7.7	1211	1.3	2.7	1181	11.5	13.4	CH2wag(53), υCC1(8)
1173(s)	1181(m)	1189	2.7	8.3	1181	10.8	6.1	1173	0.4	2.9	CH3ipr(72), υCC(8)
1161(m)	-	1150	0.5	6.6	1173	5.9	4.7	1159	189.2	39.3	βCH(59), υCC(15)
1112(m)	1115(w)	1115	3	2.5	1115	0	0.7	1115	0.9	3.2	CH3opr(96)
1109(m)	-	1098	90.5	12	1100	81.3	8.8	1109	6.6	0.7	βCH(63), υCC(26)
1064(m)	1065(w)	1061	21.2	1.8	1064	3.8	4.1	1065	79.5	18.7	υCC(32), υCO2(28)
1058(w)	-	1056	113.3	1.3	1052	18.3	1.1	1057	0.2	0.8	CH2tw(53), CH2tw1(18)
1007(w)	1007(w)	1002	2	2.8	1007	76.5	1	1007	86.8	1.5	υCO1(73), υCC(11)
992(m)	994(w)	980	198.5	1.5	983	0.1	0.8	992	0.7	2	CH2ro1(35),CH2ro(21)
968(m)	-	959	0.5	0.1	966	15.7	3.8	958	0.8	0.04	γCH(91), γring1(13)
-	955(w)	940	0	0.6	960	0.4	0.2	953	39.7	3.7	υCC1(38), βCCC(20)
937(s)	942(w)	925	10.1	1.5	933	0	0.1	937	0	0	γCH(84), γring1(13)
854(w)	855(w)	849	28.9	19.7	854	37.5	26.5	855	21.2	28.7	υCC1(50), CCSC1(13)
833(s)	831(w)	833	18.6	0.5	832	50.5	0.4	833	44.3	0.1	γ CH(60), γCO(18),
-	808(m)	804	10	2.7	809	9.8	36.5	805	10.1	31.3	υCC(30), βring1(22)
804(m)	-	803	62.1	2,5	804	0.2	0.8	804	0.2	0.1	γ CH(99)
-	-	794	30.4	10.4	765	16	0.1	772	19.9	0.3	CH2ro(24),CH2ro(24)
521(s)	-	521	3.4	0.6	521	29.2	0.9	521	34.3	0.7	γCC(40),τOH(30)

vs –very strong ; s – strong; m- medium; w – weak; AS- asymmetric; SS – symmetric; υ – stretching; β – in-plane bending; γ – out-of- plane bending; sc – scissoring; ro – rocking; wag – wagging; tw – twisting; sb – symmetric bending; ips – in-plane stretching; ops – out-of-plane stretching; ipb – in-plane bending; opb – out-of-plane bending; ipr – in-plane rocking; opr – out-of-plane rocking;

[a]Calculated IR intensities.,[b]Raman activity. [c]Only PED values greater than 10% are given.

and 1109 cm^{-1} in the FT-IR and at 1269 cm^{-1} in the FT-Raman spectrumof MBPAhavebeen assigned to C-H in-plane bending vibrations. The calculated values for C-H out-of-plane bending vibrations are at 959, 925, 833, 803 cm^{-1} by HF/6-31G (d, p) and at 966, 933, 832, 804 cm^{-1} by B3LYP/6-31++G (d, p) and at 958, 937, 833, 804 cm^{-1} by B3LYP/6-311++G (d, p) method. The C-H out-of plane bending vibrations observed in FT-IR at 968, 937, 833 and 804 $cm^{-1}$and in FT-Raman at 942 and 831cm^{-1} are in agreement with the theoretical values.

C-C vibrations: The ring carbon-carbon stretching vibrations occur in the region 1305±25- 1590±40 cm^{-1} [20, 16]. The C-C stretching vibrations of MBPA are observed at 1599, 1565, 1514, 1396, 1317 and 1064 cm^{-1} in the FT-IR spectrum and at 1605, 1515, 1396, 1320 and 1065 cm^{-1} in the FT-Raman spectrum. The computed wavenumber for C-C vibrations are found at 1630, 1572, 1514, 1405, 1319, 1061 cm^{-1} by HF/6-31G(d, p) method, 1599, 1551, 1514, 1397, 1320, 1064 cm^{-1} by B3LYP/6-31++G(d, p)method and at 1596, 1551, 1510, 1402, 1323, 1065 cm^{-1} by B3LYP/6-311++G(d, p) method. The observed values are in good correlation with the calculated values.

Methoxy group vibrations: The methyl vibrational band positions are most consistent when this group is attached to other carbon atoms. When the CH_3 group is directly attached to an oxygen atom, the C-H stretching and bending bands can shift position due to electronic effects [20]. This causes the O-CH_3 stretching bands to be spread over a larger region than that of the C-CH_3 group. For O-CH_3 compound, the C-H asymmetric and symmetric stretching vibrations appear in the range 3100-2900 cm^{-1} and 2900-2800 cm^{-1} respectively [21]. In the present investigation, the CH_3asymmetric stretching vibrations appear as weak bands in the FT-IR spectrum at 3028 and 2948 cm^{-1} and in the FT-Raman spectrum at 3029 cm^{-1}. The symmetric CH_3 stretching vibration is observed as a weak band in the FT-IR spectrum at 2841 $cm^{-1}$and the FT-Raman band at 2841 cm^{-1}. The theoretically computed CH_3 asymmetric and symmetric stretching vibrations assigned at 3046, 2948 and 2841 cm^{-1} by HF/6-31G(d, p) and at 3050, 2936 and 2841 $cm^{-1}$by B3LYP/6-31++G(d, p) and the bands at 3049, 2948 and 2841 cm^{-1} by B3LYP/6-311++G(d, p) method show excellent agreement with the experimental values. The asymmetric and symmetric bending vibrations of CH_3 group usually appear in the range of 1550-1410 cm^{-1} for methyl substituted benzenes [22]. In the title compound, strong and medium intensity bands appearing at 1574 and 1464 cm^{-1} in the FT-IR are assigned to CH_3 asymmetric deformation vibration. In the FT-Raman spectrum, the bands are observed at 1576 and 1463 cm^{-1}. The theoretically calculated values are at 1606, 1465 cm^{-1} by HF/6-31G(d, p) and at 1574, 1464 cm^{-1} by both B3LYP/6-311++G(d, p) and the B3LYP/6-31++G(d, p) methods coincide very well with the experimental values. The CH_3 symmetric deformations are observed at 1425 cm^{-1} in FT-IR and at 1439 cm^{-1} in the FT-Raman spectrum. The HF/6-31G (d, p), B3LYP/6-31++G (d, p) and B3LYP/6-311++G (d, p) calculations give symmetric CH_3 deformations at 1435 cm^{-1} for the title compound. The rocking vibrations of the CH_3 group have been calculated at 1189, 1115 cm^{-1} by HF/6-31G(d, p) and at 1181, 1115 cm^{-1} B3LYP/6-31++G(d, p) and at 1173, 1115 cm^{-1} by B3LYP/6-311++G(d, p) method, shows good agreement with the FT-IR and FT-Raman recorded values at 1173, 1112 cm^{-1} and 1181, 1115 cm^{-1} for MBPA respectively. A strong band is observed in the region 1300-1200 cm^{-1} due to C-O stretching vibrations [23]. In p-methoxy benzoic acid, the band at 1245 cm^{-1} is assigned to the C-O stretching vibration[24].In the title compound, a strong band assigned at 1246 cm^{-1} and 1245 cm^{-1} in the FT-IR and FT-Raman spectra for C-O stretching vibrations. The theoretical value of C-O stretching vibration is calculated at 1245 cm^{-1} by HF/6-31G(d, p) and at 1246 cm^{-1} by B3LYP/6-31++G(d, p) and at 1247 cm^{-1} by the B3LYP/6-311++G(d, p) method.

Methylene group vibrations: The CH_2 group frequencies, basically six fundamentals can be associated, namely with symmetric, asymmetric, scissoring, rocking, wagging and twisting vibrations. The methylene asymmetric stretching is found at 2980±45 cm^{-1} and the symmetric stretching at 2920±45 cm^{-1} [20]. In the MBPA molecule, the computed wavenumbers at 2966, 2936 cm^{-1} by the HF/6-31G (d, p) and B3LYP/6-31++G(d,p) methods and at 2966, 2926 cm^{-1} by the B3LYP/6-311++G(d,p) method are assigned to CH_2 asymmetric stretching vibrations. In the present work, the weak bands observed at 2966, 2936 cm^{-1} in the FT-IR and at 2985 cm^{-1} in the FT-Raman spectrum of MBPA are assigned to the CH_2 asymmetric modes of vibrations. Similarly, the symmetric stretching modes of vibration are assigned to the FT-IR bands at 2917 cm^{-1} and to the FT-Raman bands at 2954 and 2921 cm^{-1}. These wavenumbers are in good agreement with the calculated values at 2951, 2917 cm^{-1} by the HF/6-31G(d, p) and at 2948, 2917 cm^{-1} by the B3LYP/6-31++G(d, p) and at 2956 and 2917 cm^{-1} by the B3LYP/6-31++G(d, p) methods. The methylene deformation of –CH_2CH_2OH compounds absorbs in the region 1435±25 cm^{-1} with moderate intensity [25]. For both FT-IR and FT-Raman spectrum, the band at 1436 cm^{-1} is assigned to CH_2 scissoring mode by Tonannavar et al.[10].In the MBPA molecule, the δCH_2 vibrations are observed at 1406, 1240 cm^{-1} as strong and weak bands in the FT-IR and at 1406 cm^{-1} as a weak band in the FT-Raman spectrum, which agrees well with the computed wavenumbers at 1411, 1243 cm^{-1} by the HF/6-31G (d, p) and at 1406, 1241 cm^{-1} by the B3LYP/6-31++G (d, p) and at 1406, 1242 cm^{-1} by the B3LYP/6-311++G(d, p) methods. The methylene wag absorb with a weak to moderate intensity in the region 1260±90 cm^{-1} and 1360±30 cm^{-1} [26]. For the MBPA molecule, the wagging vibrational bands of CH_2 mode are observed at 1361, 1189 cm^{-1} as strong band in the FT-IR and at 1190 cm^{-1} as a medium band in the FT-Raman. The theoretically computed CH_2 wagging vibrations at 1398, 1197 cm^{-1} by the HF/6-31G (d, p) and at 1389, 1211 cm^{-1} by the B3LYP/6-31++G(d, p) method and at 1361, 1181 cm^{-1} by B3LYP/6-311++G (d, p)

method show good agreement with the experimental observation. The CH_2 twisting vibrations of MBPA are observed at 1302 cm^{-1} and 1058 cm^{-1} as medium bands in the FT-IR spectrum. The computed wavenumbers for the twisting modes are assigned at 1313, 1056 cm^{-1} by the HF/6-31G (d, p) and at 1302, 1052 cm^{-1} by the B3LYP/6-31++G (d, p) and at 1302, 1057 cm^{-1} by the B3LYP/6-311++G (d, p) method.

COOH vibrations: Vibrational analysis of carboxylic acid is made on the basis of carbonyl group and hydroxyl group. The O-H stretching is characterized by a very broad band appearing near about 3400-3600 cm^{-1}[27]. In the present study, the O-H stretching band observed at 3318 cm^{-1} in the FT-IR spectrumagrees well with the literature value[28]. This band is calculated at 3318 cm^{-1} by the HF/6-31G (d, p), B3LYP/6-31++G (d, p) and B3LYP/6-311++G(d, p) methods. The C=O stretch of carboxylic acid is identical to the C=O stretch in ketones, which is expected in the region 1740-1660 cm^{-1} [29]. In the title molecule, the $\nu_{c=o(carbonyl}$ frequency is observed at 1674 cm^{-1} in FT-IR spectrum and at 1665 cm^{-1} as strong band in FT-Raman spectrum. The calculated stretching vibration mode of the C =O(carbonyl) band for MBPA is at 1665 cm^{-1} by HF/6-31G (d, p) and at 1674 cm^{-1} by B3LYP/6-31++G(d, p) and B3LYP/6-311++G(d, p) methods. It can also be seen from the observed FT-IR spectrum that the stretching vibration mode of the strongest bandis assigned to the $\nu_{c=o(COOH)}$ at 1695 $cm^{-1}$and to the calculated value at 1695 cm^{-1} by HF/6-31G(d, p), B3LYP/6-31++G(d, p) and B3LYP/6-311++G(d, p) methods. The C-O stretching mode in carboxylic group normally appears in the frequency region 1200-1300 cm^{-1}[30]. In the title molecule, the C-O stretching vibration is observed at 1007 cm^{-1} in both IR and Raman spectra. The lowering of the frequency is due to the presence of methylene group. The intramolecular hydrogen bonding interactions and delocalization of ED from O4 to C1-O5 may cause a change in the characteristic frequency of C-O stretching mode [31].

Natural Bond Orbital (NBO) analysis: The larger the stabilization energy value, the more intensive is the interaction between the electron donors and the electron acceptors and the greater is the extent of conjugation of the whole system. The possible intensive interactions are given in Table III. There occurs a strong intermolecular hyper-conjugative interaction of LP2(O5)→π^*(C1-O4) which increases ED(0.19669e) that weakens the respective bonds C1-O4 leading to the stabilization of 41.52kcalmol^{-1}. The interactionsbetween lone pair LP2(O4) with antibondingC1-O5 result into the stabilization of 33.88kcalmol^{-1} respectively, which donates larger delocalization. This gives the evidence for the weakening of C1-O5 bond and its elongation (0.016 Å). The magnitude of charges transferred from lone pair oxygenLP2(O13) into σ*(C6-C7) and σ*(C6-C3) with the stabilization energy of 19.07 and 20.85 kcalmol^{-1} respectively. The other significant interactions which give stronger stabilization to the structure are π(C7-C8)→π^*(C11-C12), π(C11-C12)→π^*(C9-C10), π(C9-C10)→π^*(C7-C8) and π(C7-C8)→π^*(C6-O13) with energies 22.85, 22.63, 25.49 and 20.70kcalmol^{-1} respectively. These interactions are observed as an increase in electron density (ED) in C-C and C-O anti-bonding orbitals that weaken the respective bonds.

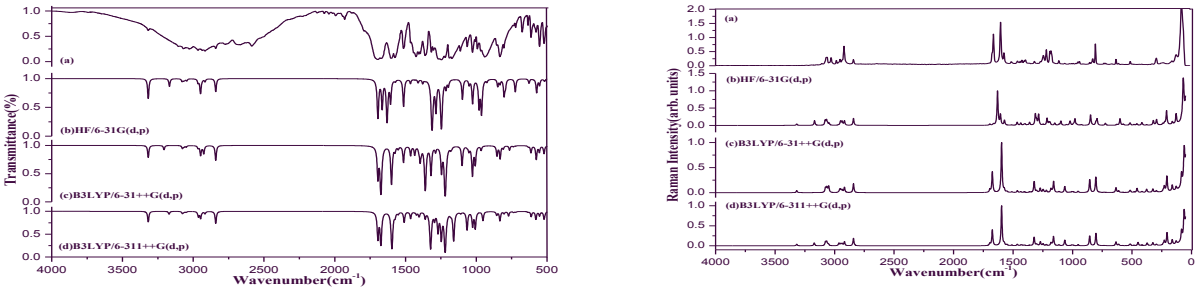

Fig. 2 (a) Experimental, (b), (c) and (d) Simulated Infrared and FT-Raman spectra of MBPA at HF/6-31G(d, p), B3LYP/6-31++G(d, p) and B3LYP/6-311++G(d, p) levels.

TableIII Second order perturbation theory analysis of fock matrix in NBO basis for MBPA

Donor(i)	ED(i)(e)	Acceptor (j)	ED (j) (e)	E(2)(kcal mol^{-1})	E(j)-E(i) (a.u)	F(i,j) (a.u)
π(C7-C8)	1.62941	π*(C6-O13)	0.15783	20.70	0.27	0.071
		π*(C9-C10)	0.39203	16.88	0.27	0.060
		π*(C11-C12)	0.29522	22.85	0.28	0.072
π(C9-C10)	1.62891	π*(C7-C8)	0.37683	25.49	0.30	0.078
		π*(C11-C12)	0.29522	14.95	0.29	0.060
π (C11-C12)	1.70568	π*(C7-C8)	0.37683	15.76	0.29	0.062

		π*(C9-C10)	0.39203	22.63	0.28	0.072
LP(2)O4	1.84483	σ*(C1-C2)	0.06554	18.68	0.63	0.099
		σ*(C1-O5)	0.10089	33.88	0.60	0.129
LP(2)O5	1.83402	π*(C1-O4)	0.19669	41.52	0.35	0.109
LP(2)O13	1.89285	σ*(C3-C6)	0.05926	20.85	0.64	0.105
		σ*(C6-C7)	0.06310	19.07	0.69	0.104
LP(1)O14	1.96347	σ*(C9-C10)	0.02998	6.95	1.10	0.078
LP(2)O14	1.82772	π*(C9-C10)	0.39203	31.92	0.34	0.098

[a]E(2) means energy of hyper conjugative interactions,[a] Energy difference between donor and acceptor i and j NBO orbitals, [c]F(i,j) is the Fock matrix element between i and j NBO orbitals

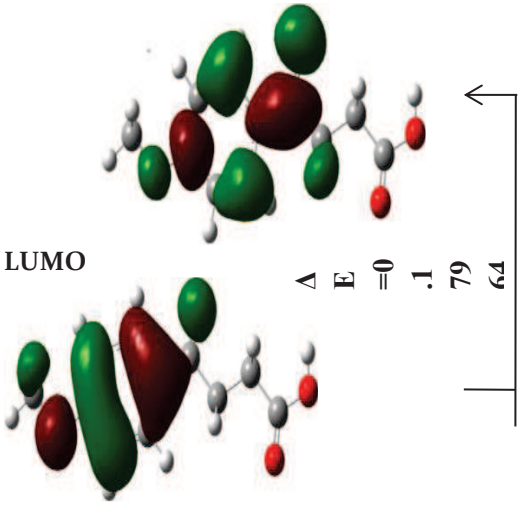

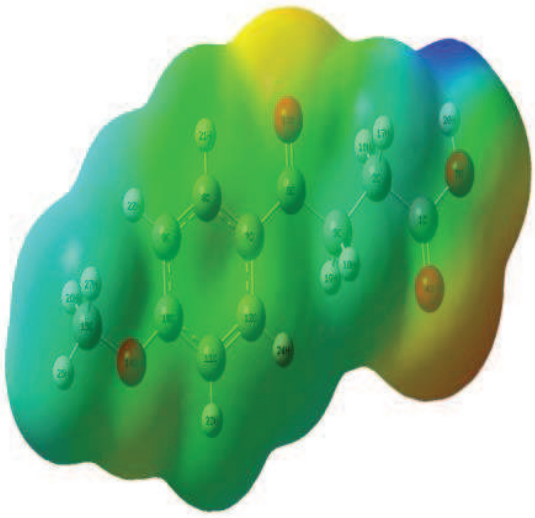

Fig.3 HOMO and LUMO plot of MBPA

Fig.4 Molecular electrostatic potential (MESP)of MBPA

Frontier Molecular Orbitals (FMOS): The HOMO and the LUMO are very important parameters for chemical reaction which examine the molecular orbital for the title molecule. The HOMO is the orbital that primarily acts as an electron donor (Highest occupied MO) and the LUMO is the orbital that acts as the electron acceptor (Lowest unoccupied MO) and the gap between HOMO and LUMO characterizes the molecular chemical stability. The energy gap between the highest occupied and the lowest unoccupied molecular orbital is a critical parameter in determining the molecular electrical transport properties because it is a measure of electron conductivity. The HOMO-LUMO energy gap of MBPA has been calculated at the B3LYP/6-311++G (d, p) level and it is 0.17964 a.u. that reflects the chemical activity of the molecules. In the title molecule, as shown in Fig.3, the HOMO→LUMO transition implies that the HOMO electrons located over the benzene ring extended with the methoxy group to the LUMO electrons exist over the benzene ring extended with the carbonyl group.

Molecular Electrostatic Potential (MESP): The MESP is a plot of electrostatic potential onto the constant electron density surface. The different values of the electrostatic potential at the surface are represented by different colours; red represents the regions of the most negative electrostatic potential, blue represents the regions of the most positive electrostatic potential and green represents the regions of zero potential. The MESP of the title compound is obtained based on the B3LYP/6-311++G (d, p) optimized result and shown in Fig.4. As can be seen from the MESP map of the title compound, while regions having the negative potential are over the electronegative atom (oxygen atoms), the regions having the positive potential are over the hydrogen atoms. It is obvious from Figure 5, that the region around oxygen atoms linked with carbon through double bond represents the most negative potential region(red). The negative regions are mainly localized on the oxygen atom of the carboxylic group with a maximum value of V(r) as -0.04769a.u.. So it is predicted that an electrophile would attack MBPA around the O4 atom. The most possible site for nucleophilic attack is on H2O, which has a maximum positive V(r) value of 0.05195a.u. Thus, the total electron density surface mapped with electrostatic potential clearly reveals the presence of high negative charge on the carbonyl oxygen(O4) in the COOH

group, while more positive charge around hydrogen atom (H20) in the COOH.

Conclusion: The molecular structural parameters and vibrational frequencies of the molecule have been determined from HF/6-31G (d, p) and DFT methods utilizing B3LYP/6-31++G (d, p) and B3LYP/6-311++G (d, p) basis sets. The NBO analysis indicates the intramolecular charge transfer between the bonding and antibonding orbitals.The magnitude of charges transferred from lone pair oxygen LP2 (O4) into π^*(C1-O5) significantly increases the population at π^*(C1-O5) causes the weakening of the bond C1-O5 and is elongated by 0.016 Å resulting in the decrease of C-O stretching frequency. HOMO-LUMO energy gap explains the eventual charge transfer interactions taking place within the molecule. Molecular electrostatic potential surface map shows regions around O4 and H20 atoms, the most possible site for electrophilic and nucleophilic attack.

References:

1. M.N. Haque, R. Chowdhury, K.M.S. Islamand, M.A. Akbar & Bang, J Anim Sci., 98 (2009) 115.
2. Renuka Sali, L.R.Naik, Mohan S, Effect of Doping Ratio on Optical Properties of 5(6) Carboxyfluorescein Doped Polystyrene Films; Engineering Sciences International Research Journal : ISSN 2320-4338 Volume 4 Issue 1 (2016) , Pg 43-45
3. Keshav, K.L. Wasewar, S. Chand & H. Uslu, Fluid Phase Equilibria, 21 (2009) 275.
4. www.linkedin.com
5. en.wikipedia.org/wiki/ibuprofen
6. M.J. Frisch., GAUSSIAN 03 Program, Gaussian, Inc.,Wattingford. CT. 2004.
7. G. Rauhut & P. Pulay, J. Phys. Chem., 99 (1995) 3093.
8. T. Sundius, VibSpectrosc., 29 (2002) 89.
9. P H Suthar, B. Y. Thakore, Concentration Dependent Electrical Transport Properties of Co-Cr Binary Alloys At Various Temperatures; Engineering Sciences International Research Journal : ISSN 2320-4338 Volume 4 Issue 1 (2016) , Pg 1-4
10. E.D. Glendening, A.E. Reed, J.E. Carpenter & F. Weinhold, NBO Version 3.1. TCI, University of Wisconsin, Medison, 1998.
11. Sajid Ali, Nasim Hassan Rama, GhulamQadeer and Ales Ruzicka, ActaCrystallographica E, 64 (2008) 02197.
12. Falleiro Sameena, Exploring Learning in New Learning Environments of the 21st Century ; Engineering Sciences International Research Journal : ISSN 2320-4338 Volume 4 Issue 1 (2016) , Pg 5-8
13. J. Tonannavar, Yashaswita Chavan andJayeshreeYenagi, Journal of International Academic Research for
14. Multidisciplinary, 3(2015)134.
15. Zhang Rui-Zhou, Li Xiao-Hong and Zhang Xian-Zhou, Indian Journal of Pure &Applied Physics,(2012) 719.
16. M.L. Vueba , International Journal of Pharmaceutics, 307(2006) 56.
17. P.Noelien Selvarani, Image Registration and Template Matching Using Wavelet Functions; Engineering Sciences International Research Journal : ISSN 2320-4338 Volume 4 Issue 1 (2016) , Pg 9-12
18. N. Sundaraganesan, B. Dominic Joshua and T. Radjakoumar, Indian Journal of pure & Applied Physics, 47(2009)248.
19. Yue Yang & HongweiGao, Spectrochim. Acta A,101 (2013) 110.
20. K. Rastogi, M.A. Palafox, R.P. Tanwar and L. Mittal, Spectrochim. Acta A,58(2002)1989.
21. Jaidev, S.S. Gill, Navneet Kaur, Performance Analysis of 20 Nm Si and GE Channel Based Pentagonal and Trapezoidal NWT; Engineering Sciences International Research Journal : ISSN 2320-4338 Volume 4 Issue 1 (2016) , Pg 13-17
22. G. Varsanyi, Vibrational spectra of Benzene Derivatives, Academic Press, New York, 1969.
23. Mehmet Karaback, Mehmet Cinar and Mustafa Kurt, Spectrochim. Acta A 74(2009)1197.
24. D.I. Pavia, G.M. Lampman, G.S. Kriz & J. Vondeling (Eds.). Introduction to Spectroscopy, third edn.,Thomson Learning, 2001, p. 579.
25. Manoj Chopra, Security Issue of Cloud Computing In E-Commerce Sector; Engineering Sciences International Research Journal : ISSN 2320-4338 Volume 4 Issue 1 (2016) , Pg 18-22
26. J. Coates, Interpretation of Infrared Spectra, a practical approach, in: R. A. Meyers (Ed.), Encyclopedia of Analytical Chemistry, John Wiley & Sons Ltd., Chichester, 2000.
27. N.P.G. Roeges, A Guide to complete Interpretation of the Infrared Spectra of Organic Structures, Wiley, New York. 1954
28. Amit Botke, Gourav Pathak, New Scopes In Artificial Neural Network; Engineering Sciences International Research Journal : ISSN 2320-4338 Volume 4 Issue 1 (2016) , Pg 23-28
29. N. Sundaraganesan, K. Sathesh Kumar, C. Meganathan & B. Dominic Joshua, Spectrochim. Acta A,65 (2006) 1186.
30. J.M.S. Green, D.J. Harrison & W. Kynoston, Spectrochim.Acta A, 27 (1971) 807.

31. Sharmistha Bhattacharya (Halder), Purnendu Das, Sanju Das, Saptarshi Paul, A Color Image Coding/Decoding Method Based on Newly Constructed Fuzzy Transforms; Engineering Sciences International Research Journal : ISSN 2320-4338 Volume 4 Issue 1 (2016) , Pg 29-33
32. J. Abkowicz-Bienko, D.C. Bienko & Z. Latajka, J. Mol.Struct., 552 (2000) 165.
33. S. Mohan, N. Puviarasan and D. Arul Dhas, Asian Journal of Chemistry, Vol 10, No. 4(1998)758.
34. N.B. Colthup, L.H. Daly & S.E. Wiberly, Introduction to Infrared Raman Spectroscopy, Academic Press, New York, 1990.
35. A.E. Ledesma, J. Zinczuk, A. BenAltabef, J.J. Lopez – Gonzalez & S.A. Brandan, J. Raman Spectroscopy,Vol.40(8) (2009) 1004.
36. Ishwar Naik, Rajashekhar Bhajantri, Spectrally Tuned P- N Junction Blend For Plastic Solar Cell; Engineering Sciences International Research Journal : ISSN 2320-4338 Volume 4 Issue 1 (2016) , Pg 34-36
37. R.M. Silverstein & F.X. Webster, Spectrometric identification of Organic compounds, sixth ed. John Wiley & Sons Inc., New York, 2003.
38. J. Clemy Monicka and C. James, Spectrochim.Acta A, 78(2011)718.
39. D.L.Vein, N.B. Colthup, W.G. Fateley & J.G. Grasselli, The Handbook of Infrared and Raman Characteristic Frequencies of Organic molecules, Academic Press, San Diego, 1991.
40. Dr. Samudrala Venkateswarlu, An Optimize Utilization of Carrier Channels for Secure Data Transmission, Retrieval and Storage in Distributed Cloud Network Using Key Management With Genetic Algorithm ; Engineering Sciences International Research Journal : ISSN 2320-4338 Volume 4 Issue 2 (2016), Pg 134
41. J. Swaminathan, M. Ramalingam, V. Sethuraman, N. Sundaraganesan, S. Sebastian and M. Kurt, Spectrochim.Acta A, 75 (2010) 183.
42. T. JoselinBeaula and C. James Spectrochim.Acta A, 122 (2014) 661.
43. Umang Shukla, Paresh Solanki, Data Perturbation Using Randomization Approach In Data Stream Mining; Engineering Sciences International Research Journal : ISSN 2320-4338 Volume 4 Issue 1 (2016) , Pg 37-42

* **

T.Chithambarathanu
Principal, S.T.Hindu College, Nagercoil
ManonmaniamSundaranar University, Tirunelveli. Tamil Nadu

K.Vanaja, J.DaisyMagdeline
Associate Professor of Physics
Rani Anna Govt College, Tirunelveli
ManonmaniamSundaranar University, Tirunelveli, Tamil Nadu